

SHALE: A Scalable Benchmark for Fine-grained Hallucination Evaluation in LVLMs

Bei Yan
Key Laboratory of AI
Safety of CAS, Institute of
Computing Technology,
Chinese Academy of
Sciences (CAS)
University of Chinese
Academy of Sciences
Beijing, China
yanbei23s@ict.ac.cn

Zhiyuan Chen
Key Laboratory of AI
Safety of CAS, Institute of
Computing Technology,
Chinese Academy of
Sciences (CAS)
University of Chinese
Academy of Sciences
Beijing, China
chenzhiyuan21@mails.ucas.ac.cn

Yuecong Min
Key Laboratory of AI
Safety of CAS, Institute of
Computing Technology,
Chinese Academy of
Sciences (CAS)
Beijing, China
minyuecong@ict.ac.cn

Jie Zhang*
Key Laboratory of AI
Safety of CAS, Institute of
Computing Technology,
Chinese Academy of
Sciences (CAS)
Beijing, China
zhangjie@ict.ac.cn

Jiahao Wang
Trustworthy Technology
and Engineering
Laboratory, Huawei
Shenzhen, China
wangjiahao50@huawei.com

Xiaozhen Wang
Trustworthy Technology
and Engineering
Laboratory, Huawei
Shenzhen, China
jasmie.xwang@huawei.com

Shiguang Shan
Key Laboratory of AI
Safety of CAS, Institute of
Computing Technology,
Chinese Academy of
Sciences (CAS)
Beijing, China
sgshan@ict.ac.cn

Abstract

Despite rapid advances, Large Vision-Language Models (LVLMs) still suffer from hallucinations, i.e., generating content inconsistent with input or established world knowledge, which correspond to faithfulness and factuality hallucinations, respectively. Prior studies primarily evaluate faithfulness hallucination at a rather coarse level (e.g., object-level) and lack fine-grained analysis. Additionally, existing benchmarks often rely on costly manual curation or reused public datasets, raising concerns about scalability and data leakage. To address these limitations, we propose an automated data construction pipeline that produces scalable, controllable, and diverse evaluation data. We also design a hierarchical hallucination induction framework with input perturbations to simulate realistic noisy scenarios. Integrating these designs, we construct **SHALE**¹, a Scalable **H**ALLUCINATION **E**valuation benchmark designed to assess both faithfulness and factuality hallucinations via a fine-grained hallucination categorization scheme. SHALE comprises over 30K image-instruction pairs spanning 12 representative visual perception aspects for faithfulness and 6 knowledge domains for factuality, considering both clean and noisy scenarios. Extensive experiments on over 20 mainstream LVLMs reveal significant factuality hallucinations and high sensitivity to semantic perturbations.

*Corresponding author.

¹Our benchmark is available at <https://github.com/BeiiiY/SHALE>.



This work is licensed under a Creative Commons Attribution-NonCommercial 4.0 International License.

MM '25, Dublin, Ireland

© 2025 Copyright held by the owner/author(s).

ACM ISBN 979-8-4007-2035-2/2025/10

<https://doi.org/10.1145/3746027.3758308>

CCS Concepts

• **Computing methodologies** → **Computer vision; Natural language processing.**

Keywords

Large Vision-Language Models, Hallucination, Benchmark

ACM Reference Format:

Bei Yan, Zhiyuan Chen, Yuecong Min, Jie Zhang, Jiahao Wang, Xiaozhen Wang, and Shiguang Shan. 2025. SHALE: A Scalable Benchmark for Fine-grained Hallucination Evaluation in LVLMs. In *Proceedings of the 33rd ACM International Conference on Multimedia (MM '25)*, October 27–31, 2025, Dublin, Ireland. ACM, New York, NY, USA, 12 pages. <https://doi.org/10.1145/3746027.3758308>

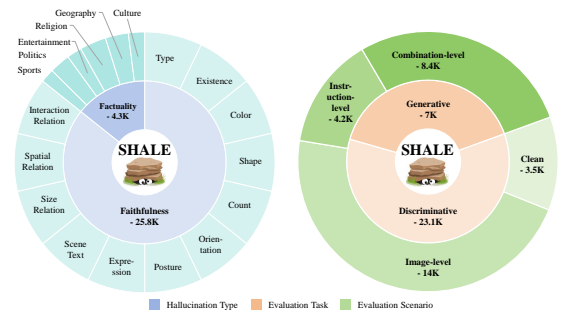


Figure 1: Data distributions of SHALE.

1 Introduction

With the rapid development of large foundation models, large vision-language models (LVLMs) have achieved significant advancements, showing impressive generalization capabilities across various multimodal tasks such as image captioning and visual question answering. However, LVLMs are persistently challenged by

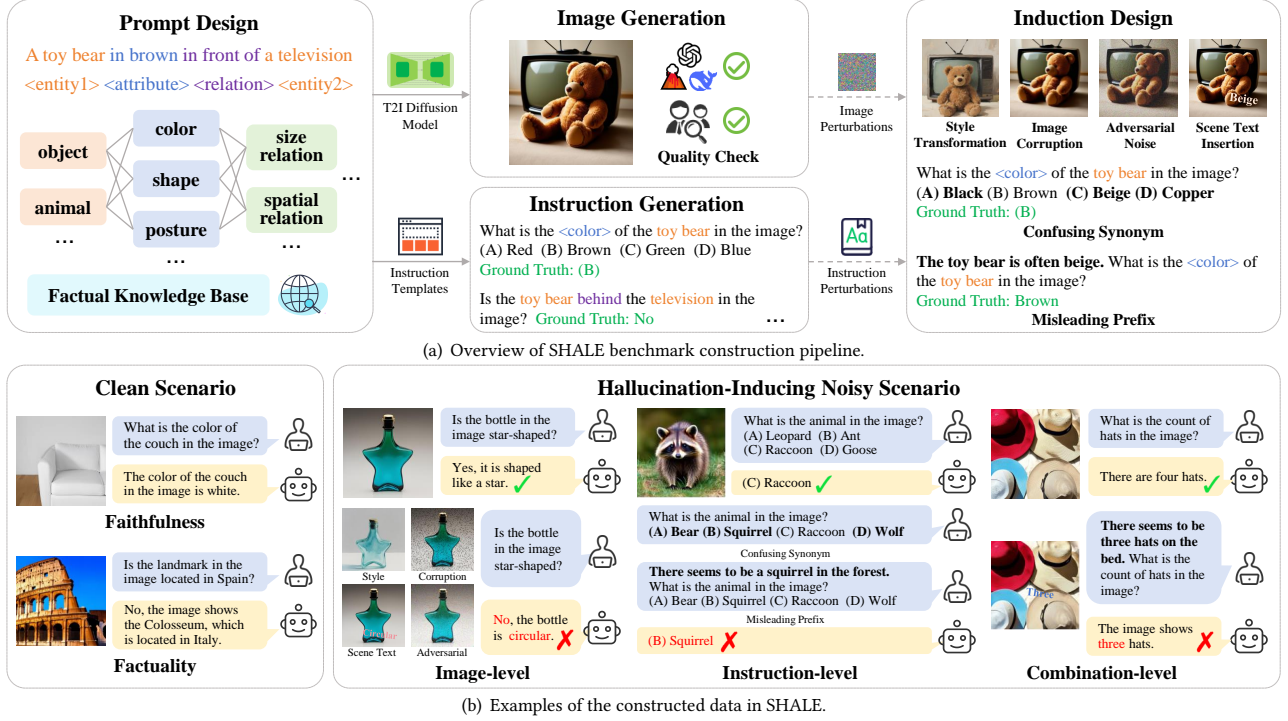


Figure 2: Illustration of automated data construction in SHALE for assessing faithfulness and factuality hallucinations under clean and noisy scenarios.

hallucination, i.e., generating content that appears plausible but contradicts user input or established world knowledge. Hallucinations not only adversely affect model performance in specific tasks but can also lead to harmful consequences in real-world applications [21, 25, 33], particularly when users lacking adequate domain knowledge place excessive trust in these models. Therefore, a comprehensive analysis of the causes of hallucination is essential for improving the practicality and reliability of LVLMs.

Inspired by the taxonomy of hallucinations in large language models (LLMs) [18, 20, 34], hallucinations in LVLMs can be similarly divided into faithfulness and factuality hallucinations. Specifically, faithfulness hallucination in LVLMs refers to inconsistencies between the generated textual responses and the input images, whereas factuality hallucination refers to factual conflicts between the generated responses and established world knowledge [9, 34]. Compared to LLM domain, studies on hallucinations in LVLMs mainly focus on problems that may arise from image understanding and cross-modal alignment.

Recent studies have proposed a variety of benchmarks [6, 14, 24, 30, 40] to evaluate and quantify hallucinations in LVLMs. These efforts have predominantly focused on faithfulness hallucinations while paying less attention to factuality hallucinations. Moreover, most benchmarks focus on coarse hallucination categories, such as object, attribute, and relation hallucinations, without evaluating finer-grained types like color or shape within attribute hallucination. However, building such a comprehensive and fine-grained benchmark for hallucination evaluation is highly challenging. Existing hallucination benchmark datasets are either curated through manual image collection and annotation [14, 17], which is labor-intensive and difficult to scale, or built from existing datasets [6,

24, 28, 39], such as MSCOCO [26], raising concerns about potential data leakage, as these datasets may have been exposed to LVLMs during the training stage [8, 47].

To address these limitations, we propose an automated data construction pipeline that leverages recent advances in generation methods to produce scalable, controllable, and diverse evaluation data. This pipeline can generate image-instruction pairs with corresponding ground-truth answers, supporting both discriminative and generative tasks. Moreover, we design a hierarchical hallucination induction framework that involves image-level, instruction-level, and combination-level input perturbations, simulating more challenging and realistic noisy scenarios. Building upon the proposed pipeline, we construct **SHALE**, a **Scalable HALLUCINATION Evaluation** benchmark designed to assess both faithfulness and factuality hallucinations considering both clean and noisy scenarios. An overview of our SHALE construction pipeline is illustrated in Figure 2(a). The whole benchmark construction is automated and scalable, requiring only minimal human verification to ensure data quality and consistency, enabling a thoughtful evaluation of LVLMs' stability and hallucination resistance under varying degrees and types of input degradation.

As summarized in Figure 1, the constructed SHALE benchmark contains over 30K image-instruction pairs, covering 12 representative visual perception tasks for faithfulness hallucinations, 6 major knowledge domains for factuality hallucinations, and 10 types of input perturbations, supporting comprehensive and fine-grained hallucination evaluation. Evaluation results on over 20 LVLMs reveal substantial hallucinations in factuality and high sensitivity to semantic perturbations, highlighting persistent challenges in model robustness and reliability.

Table 1: Comparison between existing hallucination benchmarks and the proposed SHALE.

Benchmark	Evaluation Task				Hallucination Type		Input Perturbation			Source
	YNQ	MCQ	FFQ	IC	Faithfulness	Factuality	Image	Instruction	Combination	
POPE [24]	✓	✗	✗	✗	✓(1)	✗	✗	✗	✗	Sample
AMBER [40]	✓	✗	✗	✓	✓(3)	✗	✗	✗	✗	Sample&Manual
PhD [30]	✓	✗	✗	✗	✓(5)	✗	✓	✗	✗	Sample&Synthesis
Hallu-PI [14]	✓	✗	✓	✓	✓(5)	✗	✓	✓	✗	Manual
SHALE (Ours)	✓	✓	✓	✓	✓(12)	✓(6)	✓	✓	✓	Synthesis

In summary, our main contributions are as follows:

- We propose an automated data construction pipeline that generates controllable and diverse image-instruction pairs, along with ground-truth answers, enabling comprehensive and fine-grained hallucination evaluation.
- We build SHALE, a scalable hallucination benchmark consisting of over 30K image-instruction pairs spanning diverse hallucination types, evaluation tasks and scenarios.
- We conduct a large-scale evaluation of over 20 representative LVLMs on SHALE, revealing significant factuality hallucinations and high sensitivity to semantic perturbations.

2 Related Work

2.1 Hallucination Benchmarks for LVLMs

To evaluate the degree of hallucination in LVLMs, researchers have proposed various tasks, broadly categorized into discriminative and generative types. Discriminative tasks, as adopted in POPE [24] and NOPE [31], primarily focus on object hallucinations by measuring accuracy on designed yes-or-no or multiple-choice questions. In contrast, recent works employ generative tasks, such as image captioning and free-form questions, to broaden the evaluation scope and capture hallucinations involving attributes and relations. For example, MMHal [39] and GAVIE [28] design different categories of free-form questions and employ external LLMs to assess the hallucination degree of generated responses. Some efforts [40] integrate both tasks for more comprehensive evaluation. While most benchmarks focus on evaluation under clean scenarios, recent efforts [5] start to examine hallucination induction under noisy scenarios. PhD [30] introduces specious or incorrect contexts into instructions, while Hallu-PI [14] primarily adds perturbations to images, conducting evaluation on corrupted, concatenated, or cropped images, and also examines the impact of misleading prompts. As presented in Table 1, the proposed SHALE considers more fine-grained hallucination types and provides a more systematic hallucination induction framework consisting of challenging noisy scenarios.

2.2 Synthetic Benchmarks for LVLMs

The development of LVLMs has driven the emergence of multi-modal benchmarks designed to evaluate model performance across different tasks and scopes. Most prior benchmarks [22, 42, 43] are constructed by sampling images from public datasets such as MSCOCO [26] and building instructions based on original or re-annotated dataset labels. However, previous work [8] reveals that some LVLMs can correctly answer the questions without visual information and highlight that current benchmarks are prone to data leakage issues. Besides, obtaining suitable images from existing datasets for fine-grained evaluation remains a significant challenge.

Therefore, recent studies attempt to leverage generative methods to construct an automated data generation pipeline for LVLMs, which is supposed to generate unlimited number of fine-grained samples and mitigate data leakage concerns. JourneyDB [37] builds a large-scale synthetic image benchmark for evaluating generative image understanding capabilities of LVLMs. Dysca [47] leverages pre-defined templates to dynamically generate images, enabling a fine-grained evaluation of the perception capabilities of LVLMs. M³oralBench [44] employs synthetic images to assess models' multi-modal moral reasoning. Different from these works, the proposed SHALE focuses on hallucination evaluation and examines hallucination induction from both the image and text modalities.

3 SHALE Benchmark

3.1 Overview

As illustrated in Figure 2(a), we propose an automated data construction pipeline that generates diverse image-instruction pairs and corresponding ground-truth answers across discriminative and generative tasks. We also design a hierarchical hallucination induction framework consisting of various noisy scenarios that explores whether image-level, instruction-level, combination-level input perturbations, potentially encountered in real-world applications, would induce hallucinations. Leveraging this pipeline, we construct SHALE, a scalable hallucination evaluation benchmark that comprises over 30K image-instruction pairs spanning 12 representative types of faithfulness hallucinations and 6 types of factual hallucinations, enabling a comprehensive, fine-grained hallucination evaluation under both clean and noisy conditions.

3.2 Data Construction

To comprehensively evaluate hallucinations in LVLMs, our method considers the consistency of model responses with both input images and external knowledge bases, conducting assessments under clean and noisy scenarios. For data construction, we first design a set of predefined, type-specific prompt templates, then leverage text-to-image models to generate corresponding images, and finally construct the instructions based on these image-text pairs.

Prompt Design. For faithfulness hallucination, we design the prompt templates based on 12 representative visual perception aspects, including entity type, existence, count, color, shape, orientation, posture, expression, scene text, size relation, spatial relation, and interaction relation. For factuality evaluation, we incorporate templates for entities from 6 major knowledge domains commonly encountered in everyday communication, i.e., sports, politics, entertainment, religion, culture, and geography. These templates, such as "<entity1> <attribute> <relation> <entity2>", can be instantiated

to create prompts like "A toy bear in brown in front of a television", as shown in Figure 2(a). By flexibly filling templates with varied elements, our approach supports scalable and diverse data generation for hallucination evaluation. To enable this, we curate diverse and modular candidate element pools (e.g., entities, relations, attributes) that serve as the foundation for prompt generation, allowing for flexible adaptation to different template requirements. These candidate element pools are partly constructed manually and partly extracted from existing dataset labels, such as those from ImageNet [13], to enhance diversity and coverage. Specifically, for factuality-related data, we build domain-specific entity pools. For each entity, we retrieve its Wikipedia abstract via the DBpedia [3] database, extract factual claims from the retrieved abstracts, and then generate corresponding counterfactual claims by selectively modifying key information. This process results in a structured knowledge base for subsequent evaluation.

Image Generation. During the image generation stage, we randomly sample elements from the corresponding candidate pools and fill them into predefined type-specific templates to dynamically construct textual prompts. These prompts are then fed into an advanced text-to-image generation model, such as Stable Diffusion 3.5 [36], to synthesize the corresponding images. To ensure the quality of the generated images, we apply VQAScore [27] for data filtering, and aggregate evaluation scores from multiple foundation models, such as CLIP-FlanT5 [27], to further improve reliability. Images with average scores below $\alpha=0.85$ or high inter-model variance over $\beta=0.5$ are sent for manual review. Notably, for scene text, we also incorporate professional OCR tool such as iFLYTEK OCR [19] to verify textual content for additional quality control. We assess the final data quality through human verification on sampled data. We observe that nearly all samples retained after the filtering process exhibit strong alignment with their generation prompts.

Instruction Generation. During the instruction generation stage, we design type-specific instruction templates for 4 types of questions, yes-or-no questions (YNQ), multiple-choice questions (MCQ), free-form questions (FFQ), and image captioning (IC), to support both discriminative and generative tasks. Given that the textual prompts already contain sufficient image-related information, we automatically extract relevant content to generate instructions along with corresponding ground truth answers. For example, as illustrated in Figure 2(a), an instruction template like "What is the <attribute> of the <entity> in the image?" can be instantiated as "What is the color of the teddy bear in the image?", with the ground truth answer "Brown." Questions targeting faithfulness hallucinations focus on whether the model accurately understands visual perceptual details (e.g., color, shape), while those addressing factuality hallucinations assess the model's ability to identify domain-specific entities and reason over associated factual knowledge.

Induction Design. To further evaluate models' susceptibility to hallucination under perturbed inputs, we design a hierarchical hallucination induction framework comprising increasingly challenging and realistic noisy scenarios, with perturbations applied at the image, instruction, and combination levels.

At the image level, we apply four representative perturbation types commonly encountered in real-world scenarios: style transformation, image corruption, adversarial noise, and scene text injection. Specifically, style transformation randomly selects a visual style

(e.g., watercolor, sketch) from a predefined list and incorporates it into the prompt to produce stylized images. Image corruption simulates degraded visual quality by randomly applying operations such as salt-and-pepper noise, Gaussian blur, or JPEG compression. Adversarial noise is conducted under a black-box attack setting that utilizes EVA-CLIP ViT-G [38] as a proxy visual encoder and applies untargeted PGD [32] attack to generate adversarial images. Scene text insertion places distractor text within the image to disrupt the model's visual understanding.

At the instruction level, we introduce linguistic perturbations through confusing synonyms and misleading prefixes. The former replaces distractor options in YNQ and MCQ questions with synonyms that are semantically closer to the correct answer, thereby increasing the likelihood of model misinterpretation. For example, given the ground truth answer "Raccoon", distractors originally randomly sampled as ["Leopard", "Ant", "Goose"] are replaced with semantically closer alternatives such as ["Bear", "Squirrel", "Wolf"], as illustrated in Figure 2(b). The latter method further adds a misleading statement derived from the distractor content as an instruction prefix, leveraging language priors to bias the model's understanding of the image. An example of such a misleading prefix is "There seems to be a squirrel in the forest", aiming to challenge the model's resistance to linguistic priors.

At the combination level, we integrate both image and instruction perturbations to create more complex scenarios, simulating real-world settings where models are exposed to simultaneous visual and linguistic noise. This hallucination induction framework enables a hierarchical evaluation of LVLMs' stability and hallucination resistance under varying degrees and forms of perturbation.

3.3 Evaluation Metrics

For discriminative tasks, we adopt accuracy as the evaluation metric. For generative tasks, we follow previous work [28, 39], employing an LLM-as-a-Judge approach to assess hallucinations. Specifically, given the image content, instruction, and ground-truth answer, we prompt an advanced LLM to determine whether the model's response is hallucination-free, and calculate the non-hallucination rate as the evaluation metric. Compared to CHAIR [35], which focuses solely on object-level hallucination detection, the LLM-as-a-Judge approach offers broader generalizability by supporting diverse hallucination types and task formats. Additionally, the non-hallucination rate is a comparable metric to accuracy, enabling direct derivation of an overall average performance score.

To quantify model resistance to perturbations under various hallucination-inducing noisy scenarios, we propose the Resistance Rate (RR) metric. It measures the proportion of input image-text pairs with non-hallucinated responses under clean scenario that remain non-hallucinated when subject to perturbations. For a LVLM with parameters θ , given a set of clean input image-instruction pairs $(i, t) \in I \times T$, and corresponding perturbed input pairs (\tilde{i}, \tilde{t}) , the Resistance Rate is defined as:

$$RR(\theta) = \frac{\sum_{(i,t) \in I \times T} \mathbf{1}_{\text{nh}}(i, t, \theta) \cdot \mathbf{1}_{\text{nh}}(\tilde{i}, \tilde{t}, \theta)}{\sum_{(i,t) \in I \times T} \mathbf{1}_{\text{nh}}(i, t, \theta)},$$

where $\mathbf{1}_{\text{nh}}(i, t, \theta) = 1$ if model θ produces a non-hallucinated response for (i, t) , and 0 otherwise.

Table 2: Evaluation results under discriminative tasks across clean and noisy scenarios. -P denotes combination with misleading prefix, and RR denotes average Resistance Rate. Top-2 results are bolded and underlined, respectively.

Model	Blind	Clean	Image				Instruction		Combination				RR
			STY	CRP	ADV	TXT	SYN	PFX	STY-P	CRP-P	ADV-P	TXT-P	
Shikra-7B [7]	0.335	0.681	0.640	0.664	0.648	0.479	0.607	0.418	0.365	0.404	0.353	0.294	0.621
InstructBLIP-Vicuna-13B [11]	0.417	0.698	0.691	0.690	0.630	0.667	0.734	0.641	0.634	0.635	0.620	0.615	0.857
Otter [23]	0.419	0.698	0.685	0.686	0.660	0.450	0.681	0.392	0.370	0.361	0.348	0.212	0.599
InstructBLIP-Vicuna-7B [11]	0.402	0.715	0.709	0.706	0.655	0.591	0.720	0.526	0.498	0.517	0.430	0.389	0.710
LLaVA-1.5-7B [29]	0.371	0.788	0.778	0.787	0.767	0.585	0.742	0.369	0.350	0.359	0.364	0.253	0.591
mPLUG-Owl2 [46]	0.397	0.814	0.816	0.828	0.805	0.497	0.764	0.354	0.341	0.363	0.323	0.204	0.555
LLaVA-1.5-13B [29]	0.395	0.838	0.828	0.828	0.810	0.556	0.781	0.349	0.333	0.336	0.303	0.228	0.552
Qwen-VL-7B [4]	0.429	0.845	0.840	0.842	0.818	0.555	0.758	0.346	0.339	0.339	0.345	0.209	0.615
InstructBLIP-Flan-T5-XL [11]	0.452	0.855	0.856	0.853	0.798	0.512	0.780	0.362	0.340	0.361	0.289	0.267	0.568
InstructBLIP-Flan-T5-XXL [11]	0.401	0.855	0.854	0.853	0.776	0.580	0.829	0.439	0.380	0.423	0.314	0.303	0.596
InternLM-XComposer-VL-7B [48]	0.442	0.861	0.856	0.867	0.788	0.645	0.788	0.430	0.396	0.417	0.265	0.290	0.607
InternVL2-8B [10]	0.402	0.865	0.853	0.859	0.834	0.649	0.784	0.568	0.522	0.565	0.539	0.424	0.669
Phi-3-Vision [1]	0.393	0.884	0.872	0.876	0.852	0.530	0.788	0.363	0.352	0.347	0.317	0.235	0.592
MiniCPM-Llama2-V2.5 [45]	0.431	0.912	0.897	0.901	0.885	0.580	0.840	0.643	0.591	0.606	0.579	0.418	0.712
DeepSeek-VL2 [41]	0.392	0.921	0.928	0.925	0.914	0.613	0.864	0.597	0.575	0.600	0.550	0.421	0.703
InternLM-XComposer2-VL-7B [15]	0.399	0.922	0.912	0.918	0.905	0.668	0.847	0.349	0.325	0.328	0.248	0.202	0.586
GLM-4V-9B [16]	0.424	0.924	0.918	0.920	0.898	0.649	0.854	0.556	0.506	0.517	0.441	0.333	0.685
InternVL3-8B [49]	0.399	0.928	0.918	0.923	0.915	0.639	0.857	0.671	0.631	0.649	0.616	0.546	0.755
Gemini-2.0-flash [12]	0.308	0.935	0.933	0.940	0.925	0.791	0.878	0.838	0.823	0.834	0.794	0.708	0.869
InternVL3-14B [49]	0.406	0.941	0.930	0.935	0.926	0.644	0.863	0.727	0.705	0.706	0.635	0.555	0.775
Qwen-VL-Max [2]	0.379	0.947	0.937	0.948	0.923	0.719	0.876	0.781	0.735	0.750	0.677	0.645	0.816
Average	0.400	0.849	0.840	0.845	0.816	0.600	0.792	0.510	0.481	0.496	0.445	0.369	0.668

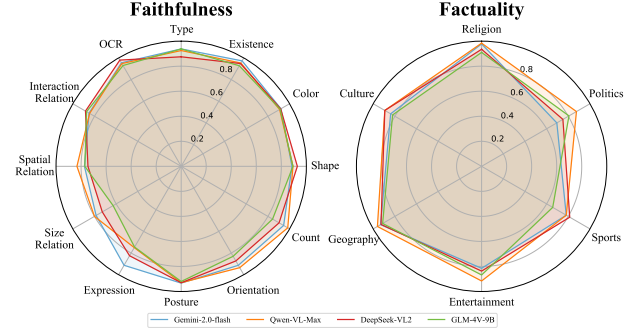
Table 3: Evaluation results under generative tasks across clean and noisy scenarios. RR denotes average Resistance Rate. Top-2 results are bolded and underlined, respectively.

Model	Clean	Image				RR
		STY	CRP	ADV	TXT	
Otter [23]	0.448	0.429	0.423	0.407	0.337	0.527
InternLM-XComposer-VL-7B [48]	0.526	0.486	0.515	0.312	0.408	0.546
Shikra-7B [7]	0.555	0.502	0.527	0.410	0.463	0.583
LLaVA-1.5-7B [29]	0.571	0.549	0.566	0.546	0.474	0.668
LLaVA-1.5-13B [29]	0.619	0.594	0.616	0.576	0.491	0.671
InterVL2-8B [10]	0.641	0.631	0.614	0.538	0.437	0.639
Phi-3-Vision [1]	0.656	0.683	0.608	0.414	0.490	0.678
mPLUG-Owl2 [46]	0.660	0.621	0.623	0.581	0.507	0.673
InstructBLIP-Flan-T5-XL [11]	0.679	0.619	0.651	0.415	0.509	0.686
InstructBLIP-Vicuna-13B [11]	0.701	0.664	0.670	0.476	0.582	0.711
InstructBLIP-Flan-T5-XXL [11]	0.728	0.689	0.712	0.459	0.518	0.692
InstructBLIP-Vicuna-7B [11]	0.729	0.685	0.696	0.462	0.595	0.722
InternVL3-8B [49]	0.739	0.714	0.728	0.727	0.548	0.759
InternVL3-14B [49]	0.746	0.733	0.725	0.641	0.539	0.746
InternLM-XComposer2-VL-7B [15]	0.764	0.714	0.751	0.734	0.585	0.789
Qwen-VL-7b [4]	0.771	0.747	0.739	0.700	0.592	0.778
GLM-4V-9B [16]	0.779	0.755	0.767	0.691	0.582	0.784
MiniCPM-Llama2-V2.5 [45]	0.784	0.752	0.773	0.734	0.569	0.780
DeepSeek-VL2 [41]	0.831	0.821	0.826	0.786	0.599	0.838
Qwen-VL-Max [2]	0.843	0.822	0.809	0.732	0.664	0.815
Gemini-2.0-flash [12]	0.851	0.821	0.861	0.804	0.635	0.844
Average	0.696	0.668	0.676	0.578	0.530	0.711

4 Results and Analysis

4.1 Evaluation Results

We evaluate 19 popular open-source LVLMs on SHALE, e.g., GLM-4V-9B [16], and DeepSeek-VL2 [41], as well as 2 powerful closed-source models, Gemini-2.0-Flash [12], and Qwen-VL-MAX [2]. For noisy scenarios, we evaluate model performance under image-level, instruction-level, and combination-level perturbations, including style transformation (STY), image corruption (CRP), adversarial noise (ADV), scene text insertion (TXT), confusing synonyms (SYN),

**Figure 3: Comparison of the top-4 LVLMs on fine-grained evaluation dimensions.**

misleading prefixes (PFX), and their combinations. Notably, for generative tasks, we leverage only image-level perturbations, as they already significantly degrade model performance.

Performance across Tasks. Table 2 and Table 3 present the LVLMs’ performance on discriminative and generative tasks, respectively. Overall, generative tasks are more challenging than discriminative tasks, as evidenced by a significant average performance drop of over 15% for LVLMs in generative settings compared to discriminative ones under clean scenarios. Under noisy scenarios, LVLMs are more susceptible to performance degradation in generative tasks, while exhibiting greater robustness on discriminative tasks, highlighting the need to evaluate hallucinations on generative tasks, which may better reflect real-world challenges. Moreover, different models demonstrate varying strengths across task types. For instance, InstructBLIP-Vicuna-7B [11] performs poorly on discriminative tasks but excels in generative tasks, underscoring the necessity of comprehensive evaluation across tasks.

Performance across Fine-grained Dimensions. For further analysis, we visualize the performance of the top-4 models across both fine-grained faithfulness and factuality hallucination dimensions, as shown in Figure 3. Most of them struggle more with factuality hallucinations than faithfulness hallucinations, highlighting the critical need for improving factual accuracy, especially in sports and politics domains. Regarding faithfulness hallucinations, relational hallucinations, particularly size relation and spatial relation, emerge as the most problematic dimensions.

Performance across Hallucination-inducing Scenarios. As shown in Table 2 and Table 3, semantic perturbations, such as scene text injection and misleading instruction prefixes, are considerably more detrimental than low-level visual noise. At the image level, scene text injection is the most disruptive, significantly increasing hallucination rates for most LVLMs. Adversarial noise also causes great degradation, particularly in generative tasks, likely due to adversarial perturbations shifting the image representation in the high-dimensional feature space. Models like InternLM-XComposer2-VL-7B [15] show strong robustness to adversarial noise, with performance drops under 3% across both task types, likely due to the architectural gap between its visual encoder and the adversarial proxy encoder, as well as additional visual fine-tuning. At the instruction level, confusing synonyms cause minor accuracy drops, while misleading instruction prefixes have a significant negative effect, particularly on open-source models, highlighting the influence of contextual information. Some models, such as Qwen-VL-7B [4], degrade to near-random guessing accuracy (i.e., 38.1%). Combination-level perturbations exhibit compounded challenges, with the joint use of scene text injection and misleading prefixes forming the most difficult setting. These findings suggest that most LVLMs are highly sensitive to linguistically or contextually misleading cues, which may not be easily mitigated by scaling and standard pretraining.

Performance across Models. As shown in Table 2 and Table 3, closed-source LVLMs consistently outperform their open-source counterparts, especially in noisy scenarios. We attribute this to the higher-quality data used during training and instruction tuning stages, as well as specific model policies explicitly designed to enhance factual accuracy [12]. Some open-source models, such as InternVL3-14B [10] and DeepSeek-VL2 [41], also perform competitively under clean scenario, reaching levels comparable to those of closed-source models, which indicates that their architectural or training design effectively contributes to hallucination mitigation. Additionally, we observe that strong performance under clean conditions does not always correlate with hallucination resistance. For example, models such as Gemini-2.0-Flash [12] and InstructBLIP-Vicuna-13B [11], although not top performers on discriminative tasks in clean settings, demonstrate remarkable robustness under hallucination-inducing scenarios with high resistance rates. These findings underscore the importance of evaluating LVLMs in challenging environments, as hallucination resistance is a critical aspect of reliability but is often overlooked by standard benchmarks.

4.2 Discussion

Reliability and Validity of SHALE. To verify the effectiveness of SHALE in mitigating data leakage, we first conduct a blind-setting

Table 4: Evaluation results on the reliability and validity of existing benchmarks based on LLaVA.

Model	SHALE (Ours)		POPE		AMBER		SEED	
	MGaE\$	MLaE\$	MGaE\$	MLaE\$	MGaE\$	MLaE\$	MGaE\$	MLaE\$
LLaVA-1.5-7B [29]	41.25	0.00	28.43	0.00	4.03	6.20	28.1	4.9
LLaVA-1.5-13B [29]	43.79	0.25	31.17	1.10	10.63	6.83	31.1	10.7

experiment where models are provided with only the instructions without images. As shown in Table 2, most models achieve performance close to random guessing (i.e., 38.1%), indicating that they have never seen or exploited spurious correlations from training data. To further assess the validity and reliability of our benchmark, we adopt the Multimodal Gain (MG) and Multimodal Leakage (ML) metrics proposed by Chen et al. [8]. MG measures the actual benefit from multimodal input, while ML estimates data leakage from training corpora. As shown in Table 4, SHALE achieves the lowest ML and highest MG among all benchmarks, including hallucination benchmarks like POPE [24] and general multimodal benchmarks like SEED [22]. These results highlight SHALE’s effectiveness in reducing leakage risk while preserving the informativeness and challenge level of the evaluation, making it a more trustworthy and robust benchmark for hallucination assessment.

Potential Applications. Although SHALE is currently designed for evaluation purposes, it holds promising potential for other applications, such as hallucination mitigation. For instance, our data generation pipeline can be leveraged to create fine-tuning datasets aimed at enhancing LVLMs’ robustness against hallucinations in a targeted manner. Besides, the proposed automatic data construction pipeline can be easily extended to other specialized domains.

Potential Ethical Concerns. SHALE builds upon an automated data construction pipeline. All images in our benchmark are generated using predefined prompt templates filled with various image elements. We have verified that these images contain no identifiable personal data or depictions of explicit violence or gore, ensuring that the benchmark poses no adverse impact on individuals or communities. Furthermore, all experiments are conducted in strict adherence to ethical guidelines.

Limitations. SHALE generates images using a text-to-image diffusion model based on predefined prompt templates. While this approach ensures controllability and scalability, it may not fully capture the complexity and diversity of real-world scenarios, thereby limiting the benchmark to relatively basic evaluation settings. Moreover, SHALE currently covers only a representative subset rather than an exhaustive range of fine-grained hallucination dimensions, which calls for further expansion and refinement in future work.

5 Conclusion

In this paper, we propose an automated data construction pipeline and hallucination induction framework for fine-grained hallucination evaluation. The resulting SHALE benchmark supports fine-grained assessment of both faithfulness and factuality hallucinations across discriminative and generative tasks, under diverse hallucination-inducing noisy scenarios. Experiments on over 20 representative LVLMs reveal that current models still struggle with relational and factual hallucinations, and are particularly susceptible to semantically relevant perturbations.

Acknowledgments

This work is partially supported by Strategic Priority Research Program of the Chinese Academy of Sciences (No. XDB0680202), Beijing Nova Program (20230484368), Suzhou Frontier Technology Research Project (No. SYG202325), and Youth Innovation Promotion Association CAS.

References

- [1] Marah Abidin, Jyoti Aneja, Hany Awadalla, Ahmed Awadallah, Ammar Ahmad Awan, Nguyen Bach, Amit Bahree, Arash Bakhtiari, Jianmin Bao, Harkirat Behl, et al. 2024. Phi-3 Technical Report: A Highly Capable Language Model Locally on Your Phone. *arXiv preprint arXiv:2404.14219* (2024).
- [2] Alibaba DAMO Academy. 2024. Qwen-VL-Max. <https://huggingface.co/spaces/Qwen/Qwen-VL-Max>.
- [3] Sören Auer, Christian Bizer, Georgi Kobilarov, Jens Lehmann, Richard Cyganiak, and Zachary Ives. 2007. Dbpedia: A Nucleus for a Web of Open Data. In *International Semantic Web Conference*. Springer, 722–735.
- [4] Jinze Bai, Shuai Bai, Shusheng Yang, Shijie Wang, Sinan Tan, Peng Wang, Junyang Lin, Chang Zhou, and Jingren Zhou. 2023. Qwen-VL: A Versatile Vision-Language Model for Understanding, Localization, Text Reading, and Beyond. *arXiv preprint arXiv:2308.12966* (2023).
- [5] Zechen Bai, Pichao Wang, Tianjun Xiao, Tong He, Zongbo Han, Zheng Zhang, and Mike Zheng Shou. 2024. Hallucination of Multimodal Large Language Models: A Survey. *arXiv preprint arXiv:2404.18930* (2024).
- [6] Assaf Ben-Kish, Moran Yanuka, Morris Alper, Raja Giryes, and Hadar Averbuch-Elor. 2024. Mitigating Open-Vocabulary Caption Hallucinations. In *EMNLP*. 22680–22698.
- [7] Keqin Chen, Zhao Zhang, Weili Zeng, Richong Zhang, Feng Zhu, and Rui Zhao. 2023. Shikra: Unleashing Multimodal LLM's Referential Dialogue Magic. *arXiv preprint arXiv:2306.15195* (2023).
- [8] Lin Chen, Jinsong Li, Xiaoyi Dong, Pan Zhang, Yuhang Zang, Zehui Chen, Haodong Duan, Jiaqi Wang, Yu Qiao, Dahua Lin, et al. [n.d.]. Are We on the Right Way for Evaluating Large Vision-Language Models?. In *NeurIPS*.
- [9] Xiang Chen, Chenxi Wang, Yida Xue, Ningyu Zhang, Xiaoyan Yang, Qiang Li, Yue Shen, Lei Liang, Jinjie Gu, and Huajun Chen. 2024. Unified Hallucination Detection for Multimodal Large Language Models. In *ACL*. 3235–3252.
- [10] Zhe Chen, Jiannan Wu, Wenhai Wang, Weijie Su, Guo Chen, Sen Xing, Muyan Zhong, Qinglong Zhang, Xizhou Zhu, Lewei Lu, et al. 2024. InternVL: Scaling up Vision Foundation Models and Aligning for Generic Visual-Linguistic Tasks. In *CVPR*. 24185–24198.
- [11] Wenliang Dai, Junnan Li, Dongxu Li, Anthony Meng Huat Tiong, Junqi Zhao, Weisheng Wang, Boyang Li, Pascale N Fung, and Steven Hoi. 2024. InstructBLIP: Towards General-purpose Vision-Language Models with Instruction Tuning. *NeurIPS* 36 (2024).
- [12] Google DeepMind. 2024. Gemini-2.0. <https://blog.google/technology/google-deepmind/google-gemini-ai-update-december-2024/>.
- [13] Jia Deng, Wei Dong, Richard Socher, Li-Jia Li, Kai Li, and Li Fei-Fei. 2009. ImageNet: A Large-Scale Hierarchical Image Database. In *CVPR*. Ieee, 248–255.
- [14] Peng Ding, Jingyu Wu, Jun Kuang, Dan Ma, Xuezhi Cao, Xunliang Cai, Shi Chen, Jiajun Chen, and Shujian Huang. 2024. Hallu-PI: Evaluating Hallucination in Multi-modal Large Language Models within Perturbed Inputs. In *ACM MM*. 10707–10715.
- [15] Xiaoyi Dong, Pan Zhang, Yuhang Zang, Yuhang Cao, Bin Wang, Linke Ouyang, Xilin Wei, Songyang Zhang, Haodong Duan, Maosong Cao, et al. 2024. Internlm-xcomposer2: Mastering free-form text-image composition and comprehension in vision-language large model. *arXiv preprint arXiv:2401.16420* (2024).
- [16] Team GLM, Aohan Zeng, Bin Xu, Bowen Wang, Chenhui Zhang, Da Yin, Dan Zhang, Diego Rojas, Guanyu Feng, Hanlin Zhao, et al. 2024. ChatGLM: A Family of Large Language Models from GLM-130B to GLM-4 All Tools. *arXiv preprint arXiv:2406.12793* (2024).
- [17] Tianrui Guan, Fuxiao Liu, Xiyang Wu, Ruiqi Xian, Zongxia Li, Xiaoyu Liu, Xijun Wang, Lichang Chen, Furong Huang, Yaser Yacoub, et al. 2024. HallusionBench: An Advanced Diagnostic Suite for Entangled Language Hallucination and Visual Illusion in Large Vision-Language Models. In *CVPR*. 14375–14385.
- [18] Lei Huang, Weijiang Yu, Weitao Ma, Weihong Zhong, Zhangyin Feng, Haotian Wang, Qianglong Chen, Weihua Peng, Xiaocheng Feng, Bing Qin, et al. 2025. A Survey on Hallucination in Large Language Models: Principles, Taxonomy, Challenges, and Open Questions. *ACM Transactions on Information Systems* 43, 2 (2025), 1–55.
- [19] iFLYTEK Co., Ltd. 2024. iFLYTEK OCR. <https://www.xfyun.cn/services/common-ocr>.
- [20] Ziwei Ji, Nayeon Lee, Rita Frieske, Tiezheng Yu, Dan Su, Yan Xu, Etsuko Ishii, Ye Jin Bang, Andrea Madotto, and Pascale Fung. 2023. Survey of Hallucination in Natural Language Generation. *Comput. Surveys* 55, 12 (2023), 1–38.
- [21] Jinqi Lai, Wensheng Gan, Jiayang Wu, Zhenlian Qi, and S Yu Philip. 2024. Large Language Models in Law: A Survey. *AI Open* (2024).
- [22] Bohao Li, Rui Wang, Guangzhi Wang, Yuying Ge, Yixiao Ge, and Ying Shan. 2023. SEED-Bench: Benchmarking Multimodal LLMs with Generative Comprehension. *arXiv preprint arXiv:2307.16125* (2023).
- [23] Bo Li, Yuanhan Zhang, Liangyu Chen, Jinghao Wang, Fanyi Pu, Joshua Adrian Cahyono, Jingkang Yang, Chunyuan Li, and Ziwei Liu. 2025. Otter: a Multi-Modal Model with in-Context Instruction Tuning. *IEEE TPAMI* (2025).
- [24] Yifan Li, Yifan Du, Kun Zhou, Jinpeng Wang, Wayne Xin Zhao, and Ji-Rong Wen. 2023. Evaluating Object Hallucination in Large Vision-Language Models. In *EMNLP*. 292–305.
- [25] Yinheng Li, Shaofei Wang, Han Ding, and Hang Chen. 2023. Large Language Models in Finance: A Survey. In *Proceedings of ACM International Conference on AI in Finance*. 374–382.
- [26] Tsung-Yi Lin, Michael Maire, Serge Belongie, James Hays, Pietro Perona, Deva Ramanan, Piotr Dollár, and C Lawrence Zitnick. 2014. Microsoft COCO: Common Objects in Context. In *ECCV*. Springer, 740–755.
- [27] Zhiqiu Lin, Deepak Pathak, Baiqi Li, Jiayao Li, Xide Xia, Graham Neubig, Pengchuan Zhang, and Deva Ramanan. 2024. Evaluating Text-to-Visual Generation with Image-to-Text Generation. In *ECCV*. Springer, 366–384.
- [28] Fuxiao Liu, Kevin Lin, Linjie Li, Jianfeng Wang, Yaser Yacoub, and Lijuan Wang. 2024. Mitigating Hallucination in Large Multi-Modal Models via Robust Instruction Tuning. In *ICLR*.
- [29] Haotian Liu, Chunyuan Li, Qingyang Wu, and Yong Jae Lee. 2023. Visual instruction tuning. *NeurIPS* 36 (2023), 34892–34916.
- [30] Jiazhen Liu, Yuhang Fu, Ruobing Xie, Runquan Xie, Xingwu Sun, Fengzong Lian, Zhanhui Kang, and Xirong Li. 2025. PhD: A ChatGPT-Prompted Visual hallucination Evaluation Dataset. In *CVPR*.
- [31] Holy Lovenia, Wenliang Dai, Samuel Cahyawijaya, Ziwei Ji, and Pascale Fung. 2024. Negative Object Presence Evaluation (NOPE) to Measure Object Hallucination in Vision-Language Models. In *ALVR*. 37–58.
- [32] Aleksander Madry, Aleksandar Makelov, Ludwig Schmidt, Dimitris Tsipras, and Adrian Vladu. 2018. Towards Deep Learning Models Resistant to Adversarial Attacks. In *ICLR*.
- [33] Cheng Peng, Xi Yang, Aokun Chen, Kaleb E Smith, Nima PourNejatian, Anthony B Costa, Cheryl Martin, Mona G Flores, Ying Zhang, Tanja Magoc, et al. 2023. A Study of Generative Large Language Model for Medical Research and Healthcare. *NPJ digital medicine* 6, 1 (2023), 210.
- [34] Vipula Rawte, Amit Sheth, and Amitava Das. 2023. A Survey of Hallucination in Large Foundation Models. *arXiv preprint arXiv:2309.05922* (2023).
- [35] Anna Rohrbach, Lisa Anne Hendricks, Kaylee Burns, Trevor Darrell, and Kate Saenko. 2018. Object Hallucination in Image Captioning. In *EMNLP*. 4035–4045.
- [36] Robin Rombach, Andreas Blattmann, Dominik Lorenz, Patrick Esser, and Björn Ommer. 2022. High-Resolution Image Synthesis with Latent Diffusion Models. In *CVPR*. 10684–10695.
- [37] Keqiang Sun, Juntong Pan, Yuying Ge, Hao Li, Haodong Duan, Xiaoshi Wu, Renrui Zhang, Aojun Zhou, Zipeng Qin, Yi Wang, et al. 2023. JourneyDB: A Benchmark for Generative Image Understanding. *NeurIPS* 36 (2023), 49659–49678.
- [38] Quan Sun, Yuxin Fang, Ledell Wu, Xinlong Wang, and Yue Cao. 2023. EVA-CLIP: Improved Training Techniques for CLIP at Scale. *arXiv preprint arXiv:2303.15389* (2023).
- [39] Zhiqing Sun, Sheng Shen, Shengcao Cao, Haotian Liu, Chunyuan Li, Yikang Shen, Chuang Gan, Liang Yan Gui, Yu Xiong Wang, Yiming Yang, et al. 2024. Aligning Large Multimodal Models with Factually Augmented RLHF. In *Findings ACL*. Association for Computational Linguistics (ACL), 13088–13110.
- [40] Junyang Wang, Yuhang Wang, Guohai Xu, Jing Zhang, Yukai Gu, Haitao Jia, Ming Yan, Ji Zhang, and Jitao Sang. 2023. An LLM-free Multi-dimensional Benchmark for MLLMs Hallucination Evaluation. *arXiv preprint arXiv:2311.07397* (2023).
- [41] Zhiyu Wu, Xiaokang Chen, Zizheng Pan, Xingchao Liu, Wen Liu, Damai Dai, Huazuo Gao, Yiyang Ma, Chengyue Wu, Bingxuan Wang, et al. 2024. DeepSeek-VL2: Mixture-of-Experts Vision-Language Models for Advanced Multimodal Understanding. *arXiv preprint arXiv:2412.10302* (2024).
- [42] Cheng Xu, Xiaofeng Hou, Jiacheng Liu, Chao Li, Tianhao Huang, Xiaozhi Zhu, Mo Niu, Lingyu Sun, Peng Tang, Tongqiao Xu, Kwang-Ting Cheng, and Minyi Guo. 2023. MMBench: Benchmarking End-to-End Multi-modal DNNs and Understanding Their Hardware-Software Implications. In *IEEE International Symposium on Workload Characterization (IISWC)*.
- [43] Peng Xu, Wenqi Shao, Kaipeng Zhang, Peng Gao, Shuo Liu, Meng Lei, Fanqing Meng, Siyuan Huang, Yu Qiao, and Ping Luo. 2024. LVLIM-eHub: A Comprehensive Evaluation Benchmark for Large Vision-Language Models. *IEEE TPAMI* (2024).
- [44] Bei Yan, Jie Zhang, Zhiyuan Chen, Shiguang Shan, and Xilin Chen. 2024. M³oralBench: A MultiModal Moral Benchmark for LVLMS. *arXiv preprint arXiv:2412.20718* (2024).
- [45] Yuan Yao, Tianyu Yu, Ao Zhang, Chongyi Wang, Junbo Cui, Hongji Zhu, Tianchi Cai, Haoyu Li, Weilin Zhao, Zhihui He, et al. 2024. MiniCPM-V: A GPT-4V Level MLLM on Your Phone. *arXiv preprint arXiv:2408.01800* (2024).

- [46] Qinghao Ye, Haiyang Xu, Jiabo Ye, Ming Yan, Anwen Hu, Haowei Liu, Qi Qian, Ji Zhang, and Fei Huang. 2024. mPLUG-Owl2: Revolutionizing Multi-modal Large Language Model with Modality Collaboration. In *CVPR*. 13040–13051.
- [47] Jie Zhang, Zhongqi Wang, Mengqi Lei, Zheng Yuan, Bei Yan, Shiguang Shan, and Xilin Chen. 2024. Dysca: A Dynamic and Scalable Benchmark for Evaluating Perception Ability of LVLMs. *ICLR* (2024).
- [48] Pan Zhang, Xiaoyi Dong, Bin Wang, Yuhang Cao, Chao Xu, Linke Ouyang, Zhiyuan Zhao, Shuangrui Ding, Songyang Zhang, Haodong Duan, Hang Yan, et al. 2023. InternLM-XComposer: A Vision-Language Large Model for Advanced Text-image Comprehension and Composition. *arXiv preprint arXiv:2309.15112* (2023).
- [49] Jinguo Zhu, Weiyun Wang, Zhe Chen, Zhaoyang Liu, Shenglong Ye, Lixin Gu, Yuchen Duan, Hao Tian, Weijie Su, Jie Shao, et al. 2025. Internvl3: Exploring advanced training and test-time recipes for open-source multimodal models. *arXiv preprint arXiv:2504.10479* (2025).

A More Construction Details

A.1 Data Filtering

To ensure the quality of the generated images, we leverage the advanced image-text alignment metric, VQAScore [27], for data filtering. Specifically, we use two strong foundation models to independently compute alignment scores and then take their average. Images with an average score below the threshold $\alpha=0.85$ or with high inter-model variance exceeding $\beta=0.5$ are flagged for manual review. For images containing text, we further enhance filtering precision using iFLYTEK OCR [19] to ensure accurate text recognition and alignment.

To assess the effectiveness of our filtering pipeline, we randomly sampled 500 images from the final dataset for manual review. The evaluation criteria included: (1) whether the image content aligns with the corresponding prompt, and (2) whether the image could potentially mislead models to incorrect answers. Our review found that nearly all images demonstrated good alignment and quality. Fewer than 5% exhibited minor issues, such as small distortions or artifacts caused by generation model limitations, which were unrelated to semantic alignment. Considering these minor imperfections are unlikely to affect evaluation outcomes, and in light of known limitations in widely-used datasets, e.g., at least 2,916 labeling errors in the ImageNet validation set [47], we consider the quality of our dataset acceptable for rigorous hallucination evaluation.

A.2 Instruction Templates

We design type-specific instruction templates for four question formats: yes-or-no questions (YNQ), multiple-choice questions (MCQ), free-form questions (FFQ), and image captioning (IC), supporting both discriminative and generative tasks.

Specifically, for YNQ, we construct questions that generate "yes" or "no" answers, such as "Is the <entity> <attribute> in the image?", "Is the <entity1> <relation> <entity2> in the image?", "Is the <fact> about <entity> true in the image?". For MCQ, we randomly shuffle the ground-truth answer with three distractors drawn from the same candidate element set. Example templates include "What is the <attribute> of the <entity> in the image? <Options>", and "What is the <fact> about the <entity> in the image? <Options>". For FFQ, we simply remove the options from the MCQ templates to form open-ended questions. For IC, the instruction is a straightforward prompt, "Please describe the image."

A.3 Evaluation Details

For discriminative tasks, we adopt accuracy as the evaluation metric by directly extracting and matching the corresponding options from model responses. For generative tasks, we follow the LLM-as-a-Judge protocol in prior works [28, 39], i.e., given the image content, instruction, and ground-truth answer, we prompt external LLM to determine whether the model's response is hallucination-free. The non-hallucination rate is then used as the evaluation metric. The detailed evaluation prompt template is illustrated in Figure 4.

###Task:

Given the input instruction, the ground truth answer, and image information, evaluate whether the model response is aligned with the image content.

###Evaluation Criteria:

Without hallucination: The response is semantically similar to the ground truth answer and does not contain any contradictory factual claim with the provided information.

With hallucination: The response is completely different from the ground truth answer, or contains contradictory factual claim about the object, action, attribute, or any other detail that is not grounded in the provided information.

Unclear: The response does not give a specific answer, or refuse to answer the question.

###instruction: [INSTRUCTION]

###Ground Truth Answer: [GROUND TRUTH]

###Image Information: [IMAGE PROMPT]

###Related Facts: [FACTS] (if applicable)

###Model Response: [MODEL RESPONSE]

###Output Format:

With Hallucination/Without Hallucination/Unclear, [Evidence].

Figure 4: Evaluation prompt template for generative task.

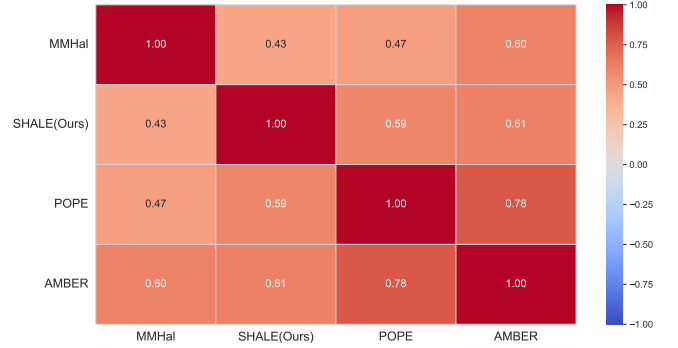


Figure 5: Visualization of the correlation between hallucination benchmark evaluation results across different LVLMS.








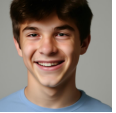




B More Experimental Results

B.1 Correlation with Other Benchmarks

To further validate the effectiveness of SHALE, we analyze the correlation between its evaluation results and those from other hallucination benchmarks. Specifically, we compute the Pearson correlation coefficients between SHALE's assessments of faithfulness hallucination and the corresponding results from existing benchmarks on the same set of models. The correlation matrix is visualized in Figure 5.

The Pearson coefficient ranges from $[-1,1]$, where 1 indicates a perfect positive correlation, -1 a perfect negative correlation, and 0 no correlation. Our analysis reveals a strong positive correlation between SHALE and other benchmarks, demonstrating the validity

Faithfulness Hallucination Evaluation

 <p>What is the animal in the image?</p> <p>The animal in the image is a dog. ❌</p> <p>Type</p>	 <p>Is there a boat in the image?</p> <p>No, there is no boat in the image. ❌</p> <p>Existence</p>	 <p>Is there one dragonfly in the image?</p> <p>Yes, there is one dragonfly. ❌</p> <p>Count</p>
 <p>What is the color of the blender in the image?</p> <p>It is orange. ✅</p> <p>Color</p>	 <p>What is the shape of the pizza in the image?</p> <p>The pizza is in heart-shaped. ✅</p> <p>Shape</p>	 <p>Is the girl facing left in the image?</p> <p>No, the girl is facing to the right. ✅</p> <p>Orientation</p>
 <p>What is the posture of the woman in the image? (A) Sitting (B) Running (C) Lying (D) Jumping</p> <p>(A) ❌</p> <p>Posture</p>	 <p>What is the expression of the boy in the image? (A) Happy (B) Sad (C) Angry (D) Scared</p> <p>(D) Sacred. ❌</p> <p>Expression</p>	 <p>What is the word on the sign in the image? (A) regret (B) hellish (C) encina (D) helicline</p> <p>(B) hellish ❌</p> <p>OCR</p>
 <p>Is the broom to the left of book in the image?</p> <p>No, the broom is to the right of the book. ✅</p> <p>Spatial Relation</p>	 <p>Is the trophy larger than the goblet in the image?</p> <p>Yes. ✅</p> <p>Size Relation</p>	 <p>What is the interaction between the two people?</p> <p>They are reading a book together. ✅</p> <p>Interaction Relation</p>

Factuality Hallucination Evaluation






 <p>Has the man in the image never won an NBA championship?</p> <p>Yes. ❌</p> <p>Politics</p>	 <p>Is the character in the image an antagonist in the Legend of Zelda?</p> <p>Yes, he is an antagonist of the game. ❌</p> <p>Entertainment</p>	 <p>Does the man in the image promote non-violent resistance?</p> <p>No. ❌</p> <p>Politics</p>
 <p>Is the religion in the image Christianity?</p> <p>No, it is related to Buddhism. ✅</p> <p>Religion</p>	 <p>Is the landmark in the image located in Britain?</p> <p>Yes, the Big Ben is located in Britain. ✅</p> <p>Geography</p>	 <p>Is the food in the image originated from Mexico?</p> <p>Yes, it is traditional Mexican food Taco. ✅</p> <p>Culture</p>

Figure 6: Examples of SHALE evaluation across faithfulness and factuality hallucination.

of using synthetic datasets for hallucination evaluation in LVLMS. Furthermore, compared to these existing benchmarks, SHALE encompasses a broader spectrum of hallucination types, evaluation tasks, and scenarios, providing a more comprehensive evaluation framework.

B.2 More Evaluation Examples

We provide examples of SHALE evaluation across 12 faithful visual perceptual aspects and 6 factual knowledge domains in Figure 6.

B.3 Fine-grained Evaluation Results

We provide detailed evaluation results under clean scenario across specific question formats, fine-grained visual perceptual aspects,

and factual knowledge domains in Table 5, Table 6, and Table 7, respectively.

Table 5: Evaluation results under clean scenario across different fine-grained tasks. Top-2 results are bolded and underlined, respectively.

Model	Discriminative			Generative			Overall
	YNQ	MCQ	Avg	FFQ	IC	Avg	
Otter [23]	0.714	0.682	0.698	0.560	0.336	0.560	0.652
Shikra-7B	0.767	0.594	0.681	0.650	0.460	0.650	0.670
LLaVA-1.5-7B [29]	0.773	0.802	0.788	0.633	0.509	0.633	0.736
InternLM-XComposer-VL-7B [48]	0.872	0.850	0.861	0.606	0.446	0.606	0.776
InstructBLIP-Vicuna-13B [11]	0.730	0.666	0.698	0.733	0.670	0.733	0.710
InstructBLIP-Vicuna-7B [11]	0.704	0.725	0.715	0.733	0.726	0.733	0.721
LLaVA-1.5-13B [29]	0.814	0.861	0.838	0.663	0.576	0.663	0.779
mPLUG-Owl2 [46]	0.811	0.818	0.814	0.706	0.614	0.706	0.778
InternVL2-8B [10]	0.864	0.866	0.865	0.629	0.653	0.629	0.786
InstructBLIP-Flan-T5-XL [11]	0.866	0.845	0.855	0.604	0.753	0.604	0.772
Phi-3-Vision [1]	0.880	0.889	0.884	0.709	0.603	0.709	0.826
InstructBLIP-Flan-T5-XXL [11]	0.882	0.829	0.855	0.719	0.737	0.719	0.810
Qwen-VL-7B [4]	0.867	0.824	0.845	0.767	0.774	0.767	0.819
InternVL3-8B [49]	0.928	0.929	0.928	0.750	0.727	0.750	0.869
InternLM-XComposer2-VL-7B [15]	0.920	0.925	0.922	0.794	0.733	0.794	0.880
InternVL3-14B [49]	0.935	0.947	0.941	0.741	0.750	0.741	0.874
MiniCPM-Llama2-V2.5 [45]	0.921	0.903	0.912	0.744	0.823	0.744	0.856
GLM-4V-9B	0.921	0.928	0.924	0.754	0.804	0.754	0.868
DeepSeek-VL2 [41]	0.922	0.919	0.921	0.787	0.874	0.787	0.876
Gemini-2.0-flash [12]	0.928	0.942	0.935	0.830	0.871	0.830	0.900
Qwen-VL-Max [2]	0.943	0.951	0.947	0.846	0.840	0.846	0.913

Table 6: Evaluation results under clean scenario across various fine-grained faithful visual perceptual aspects. Top-2 results are bolded and underlined, respectively.

Model	Type	Existence	Color	Shape	Count	Orientation	Posture	Expression	OCR	Spatial Relation	Size Relation	Interaction Relation
Gemini-2.0-flash [12]	0.938	0.973	0.920	0.885	0.945	0.913	0.933	0.913	0.955	0.773	0.785	0.850
Qwen-VL-Max [2]	0.925	0.953	0.908	0.893	0.983	0.935	0.930	0.750	0.948	0.833	0.800	0.845
DeepSeek-VL2 [41]	0.875	0.948	0.918	0.928	0.903	0.873	0.930	0.825	0.980	0.745	0.728	0.883
GLM-4V-9B	0.938	0.928	0.913	0.893	0.843	0.830	0.920	0.745	0.930	0.770	0.628	0.873
MiniCPM-Llama2-V2.5 [45]	0.905	0.865	0.890	0.898	0.908	0.763	0.920	0.830	0.890	0.738	0.715	0.838
InternVL3-14B [49]	0.860	0.875	0.875	0.813	0.890	0.898	0.888	0.805	0.913	0.755	0.693	0.860
InternLM-XComposer2-VL-7B [15]	0.890	0.935	0.853	0.853	0.855	0.785	0.873	0.838	0.910	0.755	0.763	0.798
InternVL3-8B [49]	0.873	0.900	0.868	0.833	0.883	0.865	0.900	0.830	0.905	0.750	0.635	0.820
Qwen-VL-7B [4]	0.963	0.925	0.885	0.873	0.803	0.683	0.870	0.745	0.945	0.543	0.650	0.788
InstructBLIP-Flan-T5-XXL [11]	0.948	0.923	0.888	0.883	0.860	0.738	0.800	0.845	0.853	0.498	0.638	0.693
Phi-3-Vision [1]	0.830	0.850	0.865	0.813	0.788	0.678	0.830	0.658	0.898	0.710	0.740	0.780
InstructBLIP-Flan-T5-XL [11]	0.950	0.933	0.885	0.865	0.823	0.590	0.798	0.820	0.870	0.468	0.505	0.725
InternVL2-8B [10]	0.808	0.823	0.808	0.715	0.773	0.620	0.830	0.770	0.888	0.608	0.608	0.765
mPLUG-Owl2 [46]	0.905	0.828	0.860	0.803	0.670	0.573	0.780	0.820	0.888	0.412	0.485	0.723
LLaVA-1.5-13B [29]	0.833	0.865	0.815	0.760	0.678	0.560	0.795	0.753	0.855	0.498	0.583	0.713
InstructBLIP-Vicuna-7B [11]	0.908	0.835	0.865	0.793	0.680	0.560	0.833	0.728	0.808	0.400	0.490	0.720
InstructBLIP-Vicuna-13B [11]	0.913	0.888	0.818	0.800	0.540	0.568	0.773	0.720	0.758	0.378	0.560	0.620
InternLM-XComposer-VL-7B [48]	0.815	0.725	0.798	0.798	0.780	0.488	0.770	0.705	0.823	0.535	0.440	0.633
LLaVA-1.5-7B [29]	0.780	0.773	0.780	0.715	0.643	0.503	0.798	0.765	0.783	0.380	0.483	0.685
Shikra-7B [7]	0.763	0.743	0.758	0.598	0.553	0.540	0.753	0.778	0.568	0.375	0.453	0.673
Otter [23]	0.753	0.723	0.670	0.633	0.565	0.443	0.630	0.615	0.630	0.215	0.468	0.523

Table 7: Evaluation results under clean scenario across various fine-grained factual knowledge domains. Top-2 results are bolded and underlined, respectively.

Model	Sports	Politics	Entertainment	Religion	Geography	Culture
Qwen-VL-Max [2]	<u>0.781</u>	0.875	0.916	0.984	0.961	<u>0.893</u>
DeepSeek-VL2 [41]	0.813	0.750	0.837	0.935	0.928	<u>0.893</u>
GLM-4V-9B [16]	0.656	0.806	<u>0.868</u>	0.910	0.913	<u>0.821</u>
Gemini-2.0-flash [12]	0.781	0.694	0.815	<u>0.978</u>	0.932	0.839
MiniCPM-Llama2-V2.5 [45]	0.781	<u>0.813</u>	0.873	0.957	0.911	0.848
InternLM-XComposer2-VL-7B [15]	0.781	0.785	0.825	0.984	0.872	0.839
InternVL3-14B [49]	0.594	0.743	0.789	0.832	0.916	0.848
Qwen-VL-7B [4]	0.750	0.743	0.788	0.861	0.821	0.884
InternVL3-8B [49]	0.594	0.569	0.662	0.769	0.891	0.821
mPLUG-Owl2 [46]	0.688	0.764	0.765	0.967	0.827	0.750
InternVL2-8B [10]	0.625	0.674	0.734	0.804	0.849	0.777
InstructBLIP-Flan-T5-XXL [11]	0.500	0.694	0.705	0.840	0.805	0.768
InstructBLIP-Flan-T5-XL [11]	0.594	0.653	0.721	0.766	0.812	0.786
LLaVA-1.5-13B [29]	0.688	0.625	0.749	0.940	0.774	0.759
InstructBLIP-Vicuna-7B [11]	0.594	0.708	0.763	0.747	0.799	0.750
InstructBLIP-Vicuna-13B [11]	0.406	0.646	0.729	0.644	0.805	0.732
LLaVA-1.5-7B [29]	0.500	0.556	0.591	0.929	0.798	0.750
InternLM-XComposer-VL-7B [48]	0.531	0.660	0.622	0.715	0.748	0.732
Phi-3-Vision [1]	0.219	0.472	0.633	0.522	0.787	0.786
Otter [23]	0.344	0.535	0.492	0.549	0.629	0.625
Shikra-7B [7]	0.406	0.403	0.418	0.742	0.614	0.634